

Spatiotemporal characterization of few-cycle laser pulses: erratum

Benjamín Alonso,^{1,*} Miguel Miranda,² Íñigo J. Sola,¹ and Helder Crespo²

¹Universidad de Salamanca, Grupo de Investigación en Óptica Extrema (GIOE) Pl. de la Merced s/n E-37008 Salamanca, Spain

²IFIMUP-IN and Departamento de Física e Astronomia, Universidade do Porto, R. do Campo Alegre 687, 4169-007 Porto, Portugal

*b.alonso@usal.es

Abstract: We provide the retrieved pulse for optimum wedge insertion (maximum compression) conditions and correct its time evolution due to the spectral phase having been wrongly assigned the opposite sign in our previous paper [Opt. Express **20**, 17880 (2012)]. These changes do not affect the conclusions of the paper.

©2013 Optical Society of America

OCIS codes: (320.7100) Ultrafast measurements; (320.2250) Femtosecond phenomena; (320.5520) Pulse compression; (320.7090) Ultrafast lasers.

References and links

1. B. Alonso, M. Miranda, I. J. Sola, and H. Crespo, "Spatiotemporal characterization of few-cycle laser pulses," Opt. Express **20**(16), 17880–17893 (2012).
2. M. Miranda, C. L. Arnold, T. Fordell, F. Silva, B. Alonso, R. Weigand, A. L'Huillier, and H. Crespo, "Characterization of broadband few-cycle laser pulses with the d-scan technique," Opt. Express **20**(17), 18732–18743 (2012).
3. B. Alonso, R. Borrego-Varillas, O. Mendoza-Yero, Í. J. Sola, J. S. Román, G. Mínguez-Vega, and L. Roso, "Frequency resolved wavefront retrieval and dynamics of diffractive focused ultrashort pulses," J. Opt. Soc. Am. B **29**(8), 1993–2000 (2012).

We report here corrections for reference [1]. In Section 4.1, it is said that the pulse retrieval in Figs. 4(c) and 4(d) is for the best compression achieved, whereas it actually corresponds to a non-optimal wedge position, namely the "zero" glass insertion ($d = 0$) in the corresponding d-scan traces in Figs. 4(a) and 4(b), where the pulse is still negatively chirped. Clearly, the maximum of the second-harmonic generation signal - directly related to the optimum compression conditions - appears shifted upwards in the traces, occurring for the insertion $d = 0.7$ mm. Therefore, we corrected the retrieved spectral phase with the positive dispersion introduced by the additional 0.7 mm of BK7. Also, in [1] we inadvertently used the opposite sign for the spectral phase, which has been corrected here. In Figs. 1(a) and 1(b), we give the pulse in the spectral and the temporal domains, respectively. These figures correct Figs. 4(c) and 4(d) in [1].

Notice that, as a consequence of the above corrections, the duration of the compressed pulses has now been reduced from 7.8 ± 0.1 fs to 7.3 ± 0.1 fs (FWHM) due to considering optimum compression ($d = 0.7$ mm) conditions instead of the previous "zero" glass insertion ($d = 0$). Also, the corrected spectral phase sign implies that the retrieval has in fact a post-pulse (Fig. 1(b)) instead of a pre-pulse.

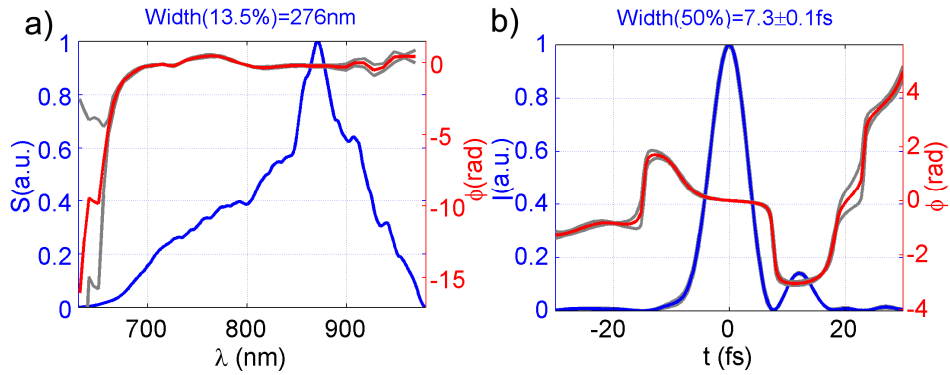


Fig. 1. Amplitude and phase of the pulse retrieval for the best achieved compression in the (a) spectral and (b) temporal domains.

These corrections do not affect the spectral amplitude and the wavefront results given in Fig. 5 of [1]. However, the results in Fig. 6 of [1] will differ. The overall spatial evolution along the focusing region is the same, although the temporal dependence of the pulse now corresponds to a shorter pulse followed by a post-pulse (the correct results are given in Fig. 2), similarly to the temporal dependence shown here in Fig. 1(b).

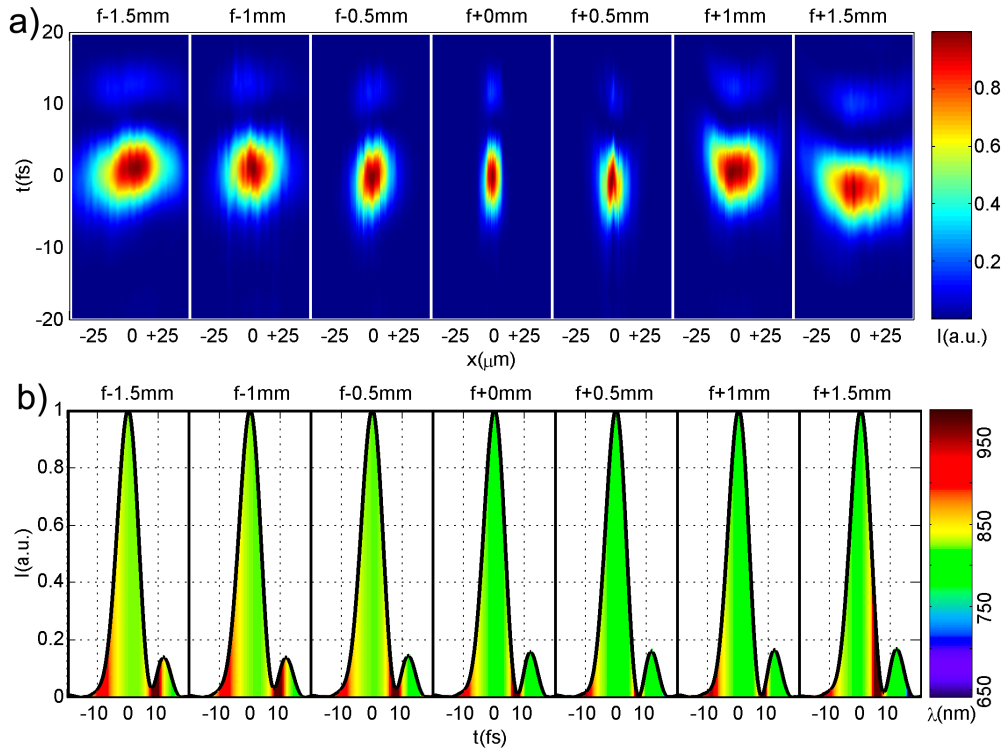


Fig. 2. (a) Normalized spatiotemporal intensity at different propagation distances z around the focus of the off-axis parabolic mirror. (b) Normalized on-axis intensity ($x = 0$) colored by the instantaneous wavelength of the pulse for the same propagation distances.

Regarding the on-axis comparison of Section 4.3, it is affected equivalently. Figure 7 in the original manuscript is corrected here by Fig. 3. Therefore, the average pulse duration on-axis is reduced from 8.0 ± 0.3 fs to 7.5 ± 0.2 fs (Fig. 3(c)). Again, the temporal profile corresponds to a post-pulse (see Figs. 3(c) and 3(d)), as obtained from the spectral phase given

in Fig. 3(a). Consequently, the on-axis pulse duration as a function of the propagation distance (red curve in Fig. 3(b)) is reduced by ~ 0.5 fs with respect to [1].

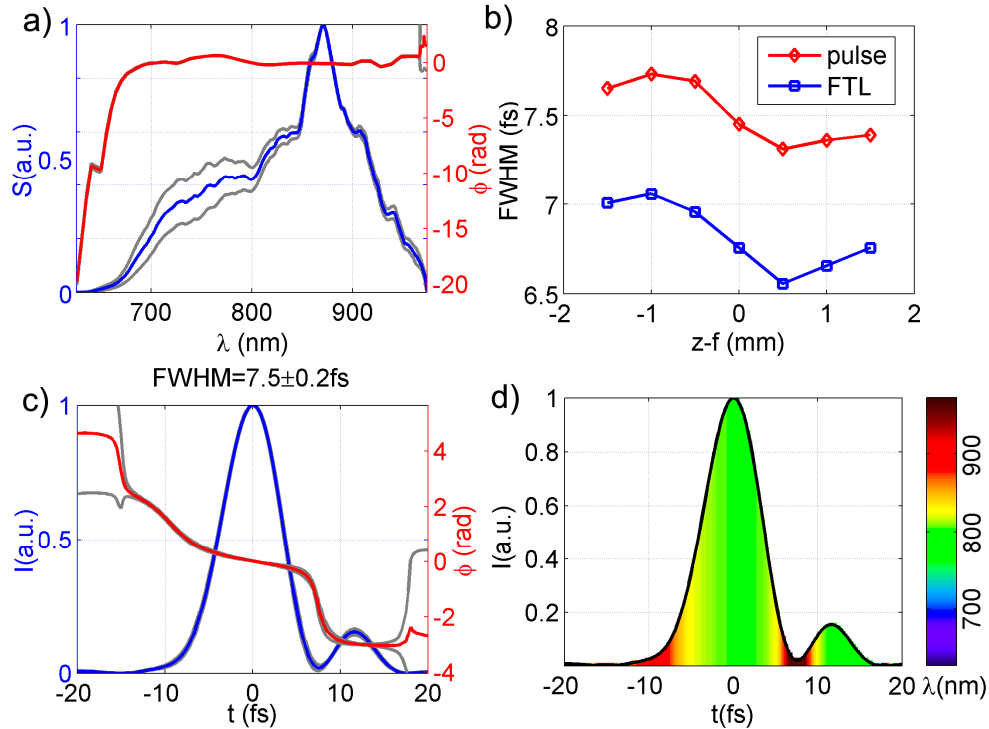


Fig. 3. (a) Mean of the spectral amplitudes (blue curve) and phases (red curve) retrieved on-axis for the seven propagation distances, and corresponding standard deviation (gray curves). (b) Temporal width (FWHM) of the on-axis intensity reconstructions of the pulses for different propagation distances, and comparison with the FWHM of the Fourier-transform limit (FTL) of the corresponding spectra. (c) Mean of the temporal amplitudes (blue curve) and phases (red curve) retrieved on-axis for the seven propagation distances, and standard deviation (gray curves). (d) Intensity colored by the instantaneous wavelength (see colorbar) of the mean of the on-axis measured pulses.

The calculated values of the peak irradiance (Section 4.4) are slightly modified due to the temporal duration correction. The correct values obtained at the focus are $\kappa_G = 7.04 \cdot 10^{10} \text{ W/cm}^2$, $\kappa_{r1} = 6.54 \cdot 10^{10} \text{ W/cm}^2$ and $\kappa_{r2} = 6.52 \cdot 10^{10} \text{ W/cm}^2$ in the Gaussian irradiance approximation, for the measured spatiotemporal irradiance from the sets $r_1 = \{x/x \geq 0\}$ and $r_2 = \{x/x \leq 0\}$, respectively. Consequently, the curves in Fig. 8 are re-scaled by these peak values.

We also would like to correct references 23 and 28 in [1], which should be references [2] and [3] in the present erratum, respectively.

We apologize for the errors in our paper [1]. These corrections are consequence only of the rectification of the spectral phase of the reference pulse and do not affect the main purpose of the paper nor its conclusions.